Degradation of IF1 controls energy metabolism during osteogenic differentiation of stem cells

María Sánchez-Aragó[1], Javier García-Bermúdez[1], Inmaculada Martínez-Reyes[1], Fulvio Santacatterina[1] and José M. Cuezva[1, *]

[1]Departamento de Biología Molecular, Centro de Biología Molecular Severo Ochoa, CSIC-UAM, Centro de Investigación Biomédica en Red de Enfermedades Raras (CIBERER), Centro de Investigación Hospital 12 de Octubre, ISCIII, Universidad Autónoma de Madrid, 28049 Madrid, Spain.

*, To whom correspondence should be addressed at: Centro de Biología Molecular, c/ Nicolás Cabrera 1, Universidad Autónoma de Madrid, 28049 Madrid, Spain. (Phone: 34911964618; Fax: 34911964420; Email: jmcuezva@cbm.uam.es)

Running Title: IF1 is a stem cell marker

Abstract

Differentiation of human mesenchymal stem cells (hMSCs) requires the rewiring of energy metabolism. Herein, we demonstrate that the ATPase Inhibitory Factor 1 (IF1) is expressed in hMSCs and in prostate and colon stem cells but is not expressed in the differentiated cells. IF1 inhibits oxidative phosphorylation and regulates the activity of aerobic glycolysis in hMSCs. Silencing of IF1 in hMSCs mimics the metabolic changes observed in osteocytes and accelerates cellular differentiation. Activation of IF1 degradation acts as the switch that regulates energy metabolism during differentiation. We conclude that IF1 is a stemness marker important for maintaining the quiescence state.

Keywords: ATPase Inhibitory Factor 1/ Cellular differentiation/ H+-ATP synthase/ Mitochondria/ Protein degradation

Introduction

A master regulator of energy metabolism in aerobic differentiated cells is the mitochondrial H^+-ATP synthase, the engine of oxidative phosphorylation (OXPHOS) that catalyzes the synthesis of ATP using as driving force the proton gradient generated by the respiratory chain. The ATPase Inhibitory Factor 1 (IF1) [1] is the physiological inhibitor of the H^+-ATP synthase that is highly overexpressed in mitochondria of cancer cells [2]. The overexpression of IF1 results in the inhibition of the ATP synthetic activity of the enzyme, the switch to an increased aerobic glycolysis [2] and the ROS-mediated signaling of several features of the oncogenic phenotype [3]. These findings supported a role for IF1 as a master regulator of energy metabolism and retrograde nuclear signaling in cancer.

Adult human mesenchymal stem cells (hMSCs) are characterized by their multi-lineage differentiation potential (pluripotency) and their self-renewal capacity [4]. Recently, the study of energy metabolism of stem cells has received attention because of its implication in nuclear reprogramming. Undifferentiated pluripotent stem cells have a low activity of mitochondrial OXPHOS and preferentially utilize aerobic glycolysis as a major source of energy supply [4]. In contrast, differentiated cells depend more heavily on OXPHOS [5, 6]. Interestingly, stemness factor-mediated nuclear reprogramming of somatic cells induces the downregulation of OXPHOS concurrently with the activation of glycolysis [7]. However, the mechanism and signaling molecule that gears the stem cell decision to change its energy metabolism and hence to onset proliferation or differentiation programs are unknown.

Here we demonstrate that the enhanced bioenergetic activity of mitochondria upon osteogenic induction is not supported by proliferation of the organelles but by the bioenergetic differentiation of pre-existing mitochondria. We show that IF1 is expressed

in hMSCs and in stem cell niches of CD44 positive cells of the human prostate and colon but is not expressed in differentiated osteocytes. Remarkably, IF1 promotes aerobic glycolysis in hMSCs and its expression is stringently regulated by degradation during osteogenic induction. Our findings support a functional role for IF1 in the regulation of stem cell fate decisions.

Results

Onset of OXPHOS upon osteogenic differentiation. Osteogenesis from hMSCs promoted a large change in cellular morphology (Fig. 1A) with concurrent upregulation of the osteogenic marker osteopontin (Fig. 1B) and down-regulation of the stem cell marker CD44 (Fig. 1B). Hence, the osteopontin/CD44 ratio, an index of osteogenic differentiation, was significantly increased in osteocytes when compared to hMSCs (Fig. 1B).

Basal rates of aerobic glycolysis were not significantly different between hMSCs and osteocytes (Fig. 1C). Inhibition of OXPHOS with oligomycin (OL) did not affect the rates of aerobic glycolysis in hMSCs (Fig. 1C) but promoted an increase in glycolysis in osteocytes (Fig. 1C). Consistently, osteocytes showed a significant increase in basal, oligomycin sensitive (OSR) and maximum uncoupled (MRR) respiratory rates (Fig. 1D). Basal cellular ATP concentrations were not significantly different between hMSCs and osteocytes (Fig. 1E). However, OL only promoted a significant decrease in ATP content in osteocytes (Fig. 1E). The drop in ATP levels in response to OL treatment in osteocytes could not be attributed to an enhanced cell death (Fig. S1) but as a result of a higher dependence of this cellular type on OXPHOS.

Osteogenic induction triggers mitochondrial differentiation. Cellular differentiation triggered a significant increase in the expression of NADH subunit 9 from complex I, succinate dehydrogenase B from complex II, core 2 from complex III, cytochrome c oxidase subunits I and II from complex IV and the α- and β-F1-ATPase subunits of the H^+-ATP synthase from complex V of OXPHOS (Fig. 2A and Fig. S2A). A concurrent decrease in the expression of the glycolytic proteins glyceraldehyde-3-phosphate dehydrogenase (GAPDH), pyruvate kinase isoform M2 (PK-M2) and lactate dehydrogenase A (LDHA) was observed (Fig. 2A and Fig. S2A). Hence, the overall mitochondrial capacity of the cell (β-F1-ATPase/GAPDH ratio) [8] (see Supplemental Information) was significantly augmented in osteocytes (Fig. S2A). Other mitochondrial proteins such as NADH Fe-S protein 3 (NDUFS3) from complex I, cytochome oxidase subunit IV from complex IV, hydroxyacyl-CoA dehydrogenase (HADHA) of β-oxidation, porin (VDAC) and the structural mitochondrial protein Hsp60 revealed no relevant changes during osteogenic induction (Fig. 2A and Fig. S2A). Analysis of OXPHOS complexes in blue native gels revealed no relevant differences in their assembly between hMSCs and osteocytes (Fig. S2B) supporting that their assembly is not limiting OXPHOS in hMSCs.

In contrast with recent findings [6] we observed that osteogenic induction occurred in the absence of relevant changes in mitochondrial DNA (mtDNA) copy number (Fig. 2B) as well as in mitochondrial mass as assessed by the cardiolipin content of the cell (Fig. 2C). Analysis of mitochondrial morphology and abundance using MitoTracker Red revealed large differences in organelle shape (Fig. 2D) and the absence of differences in mitochondrial content (histogram in Fig. 2D). Mitochondria in hMSCs were predominantly punctiform whereas the thread-like morphology was more abundant in osteocytes (Fig. 2D), in agreement with previous findings in pluripotent

stem cells [9]. High-resolution electron microscopy further confirmed no significant differences in the number of mitochondria per cell section between osteocytes and hMSCs (Fig. 2E). However, hMSCs contained a high percentage of mitochondria with abnormal structure when compared to mitochondria in osteocytes (Fig. 2E). These results indicate that osteogenic induction promotes the bioenergetic differentiation of mitochondria rather than organelle proliferation as supported by the increase in the β-F1-ATPase/Hsp60 ratio [8] (see Supplemental Information) observed in osteocytes when compared to hMSCs (Fig. 2F).

We observed no relevant differences in the expression of β-F1-ATPase mRNA between hMSCs and osteocytes (Fig. S3A) suggesting that the expression of β-F1-ATPase (Fig. 2A) is controlled at the level of mRNA translation during differentiation, what is in agreement with similar findings in development and in oncogenesis [10]. miR-127-5p targets the 3´UTR of β-F1-ATPase mRNA and inhibits its translation [11]. However, both hMSCs and osteocytes do not express significant levels of miR-127-5p (Fig. S3B) indicating that it is not involved in repressing the bioenergetic differentiation of mitochondria in hMSCs.

IF1 regulates energy metabolism of stem cells. Western blot analysis revealed that osteocytes do not express IF1 when compared to hMSCs (Fig. 3A). siRNA-mediated silencing of IF1 in hMSCs resulted in a significant reduction of the rates of aerobic glycolysis (Fig. 3B). In this situation OL treatment promoted a significant increase in lactate production (Fig. 3B). Consistently, downregulation of IF1 in hMSCs promoted an increase in the activity of the mitochondrial H^+-ATP synthase (Fig. 3C). Although basal cellular ATP concentrations were not affected by IF1 downregulation (Fig. 3D), a significant drop in cellular ATP content occurred in the presence of OL in IF1-silenced hMSCs (Fig. 3D). These results suggest that IF1 is part of the switch that

controls energy metabolism upon osteogenic induction of hMSCs (Fig. 1). The regulated expression of IF1 does not affect the proliferation rate of hMSCs (Fig. S4) in contrast to data obtained in colon cancer cells [3] suggesting a cell-type specific variability in nuclear responses to IF1 signaling.

Regulation of IF1 expression in stem cells. hMSCs and osteocytes revealed no relevant differences in the cellular content of IF1 mRNA (Fig. 3E). Twenty-four hour-treatment of hMSCs and osteocytes with AEBSF (a serine protease inhibitor) promoted a large accumulation of IF1 in both cellular types (Fig. 3F). However, the accumulation of IF1 in AEBSF-treated osteocytes exceeded by 3-fold the accumulation observed in hMSCs, suggesting that normal differentiated cells degrade IF1 at much faster rate than hMSCs. A siRNA-based screen aimed at the identification of the protease involved in the degradation of IF1 in hMSCs (Fig. S5A) and HCT116 colon cancer cells (Fig. S5B) failed to provide a candidate responsible for the degradation of IF1 despite evidence of partial silencing of the seven proteases tested (Fig. S5). Remarkably, whereas treatment of hMSCs with AEBSF did not induce significant changes in the rates of aerobic glycolysis (Fig. 3G), the same treatment in osteocytes triggered a large increase in the glycolytic flux (Fig. 3G), comparable to that induced by treatment with OL (Fig. 3G). Moreover, silencing of IF1 accelerated the rate of differentiation as revealed by the osteopontin/CD44 ratio after 12 days of osteogenic induction (Fig. 3H) suggesting a role for IF1 in signaling the repression of cellular differentiation.

IF1 is a marker of stem cells. Immunohistochemistry of IF1 revealed that it is expressed in basal epithelial cells of the prostate (Fig. 4A) and in the Lieberkühn crypts of the colon (Fig. 4A). A high expression of IF1 was also observed in prostate and colon carcinomas (Fig. 4A). Double-immunofluorescence microscopy analysis for CD44 and IF1 in human prostate and colon showed the colocalization of both markers in basal

epithelial cells and Lieberkühn crypts, respectively (Fig. 4B), which are the sites where stem cells are located in these tissues [12, 13].

Discussion

Metabolic reprogramming during cellular differentiation [4-6] or in the dedifferentiation of somatic cells into iPSC [7] or into cancer cells [3] is well established. Here we show that upon osteogenic differentiation of hMSCs there is an up-regulation of proteins of complex I, II, III, IV and V of OXPHOS. These changes result in an increase in the activity of the respiratory chain and of the H^+-ATP synthase and a higher dependence of osteocytes on OXPHOS to provide the ATP needed to sustain cellular specialization. Despite the enhancement of OXPHOS and the partial down-regulation of the cellular content of glycolytic enzymes in osteocytes, the differentiated cells still show similar rates of glycolysis as hMSCs indicating that the higher energy requirements of osteocytes cannot be covered by OXPHOS alone. Moreover, the maintenance of the glycolytic flux despite the diminished expression of glycolytic enzymes in osteocytes highlights the relevance of allosteric regulation of this metabolic pathway.

The mitochondrial phenotype of a given cell is the result of cell-type specific programs that are regulated at both the transcriptional [14] and post-transcriptional [10] levels. Transcriptional programs usually result in the onset of mitochondrial proliferation [14] whereas post-transcriptional ones promote the rapid bioenergetic differentiation of the organelle in response to changing physiological cues (for review see [10]). Our findings indicate that the enhanced activity of OXPHOS in osteocytes is not supported by an enhanced mitochondrial proliferation but by the bioenergetic differentiation of pre-existing stem cell mitochondria in agreement with findings upon

pluripotent stem cell differentiation [9, 15]. Consistently, the bioenergetic accomplishment of mitochondria during osteogenesis also seems to be regulated at post-transcriptional level [10].

Rewiring of energy metabolism to aerobic glycolysis has been shown to foster nuclear reprogramming both during oncogenesis [16] and in dedifferentiation to iPSC [7]. However, the molecule that orchestrates the metabolic switch during stem cell differentiation remains elusive. Here, we show that IF1 regulates energy metabolism of hMSCs by inhibiting the activity of OXPHOS and promoting aerobic glycolysis reproducing the effect of OL in cellular metabolism [2]. Kinetic evidence indicates that IF1 inhibits the ATP hydrolase activity of the H^+-ATP synthase [1]. However, it is likely that binding of IF1 to the H^+-ATP synthase also depends on the mass-action ratio and hence when IF1 is expressed, as it is the situation in hMSCs, it can also inhibit the synthase activity of the enzyme. Indeed, silencing of IF1 in hMSCs resulted in a drop in glycolysis and a concurrent increase in ATP synthase activity. Conversely, its overexpression in different cell types has been shown to increase glycolysis and to inhibit the ATP synthase activity, mimicking the metabolic effects triggered by the ATP synthase inhibitor OL [2, 3]. Moreover, we document the expression of IF1 in hMSCs as well as in human prostate and colon stem cells but not in osteocytes and other differentiated cells. Remarkably, disappearance of IF1 seems to be a prerequisite to facilitate the metabolic switch that accompanies cellular differentiation, emphasizing the prominent role that IF1 might play in the maintenance of stemness. However, other mechanisms might also operate since it has been reported that human pluripotent stem cells have a low content of IF1 and their differentiation is triggered by repression of UCP2 [9].

Recent findings have stressed the relevance of post-translational modification of pluripotency-associated transcription factors to simultaneously maintain pluripotency or induce lineage-specific differentiation (for review see [17]). The results in this report add on the same idea by stressing the relevance of the degradation of IF1 in maintaining energy metabolism of the undifferentiated state of stem cells. The accumulation of IF1 in response to the inhibitor AEBSF indicates that the protein is degraded by a mitochondrial serine-protease. The enhanced degradation of IF1 in osteocytes might thus result from the activation of any of these proteases as a surrogate process of the nuclear reprogramming that renders ongoing the differentiated state and/or because IF1 is experiencing a post-translational modification that makes it more susceptible to degradation. Our screening for the putative protease involved indicates that degradation of IF1 is more complex than originally anticipated and might involve an unexplored pathway for the degradation of mitochondrial proteins.

Cancer and stem cells display large phenotypic analogies regarding the molecular and functional activities of the proteins involved in glycolysis and in mitochondrial OXPHOS (Fig. 4C). The expression of IF1 represents an additional phenotypic trait in common (Fig. 4C). Deciphering the nuclear responses to the presence or absence of IF1 will certainly contribute to understand stem cell fate decisions. Overall, we show that IF1 is a stem cell marker that regulates energy metabolism of hMSCs. The regulated degradation of IF1 hinders self-renewal of stem cells to favor differentiation.

Methods

Culture of hMSC. hMSCs were obtained from Lonza and cultured according to manufacturer's instructions, for additional details see Supporting Information.

Determination of aerobic glycolysis and oxygen consumption rates. The rates of aerobic glycolysis were determined by the enzymatic determination of lactate in the medium in the absence or presence of 6 μM OL [18]. The oxygen consumption rates were determined in a XF24 Extracellular Flux Analyzer (Seahorse Biosciences) [2].

Determination of ATP. Cells were incubated for 1h in the presence or absence of 6μM OL and cellular ATP concentrations were determined using the ATP Bioluminiscence Assay Kit CLS II (Roche).

Western blot analysis. Cellular lysates were processed for blotting as indicated [2]. Details of the antibodies used are provided in Supporting Information.

Determination of mtDNA copy number. After cellular DNA extraction the quantification of mtDNA (mtDNA/nDNA) was performed by qPCR using the LightCycler® 2.0 Real-Time PCR System as described [19].

Electron microscopy. For ultrastructural studies, hMSC and osteocytes were fixed with 2% glutaraldehyde in 0.1M Sörensen phosphate buffer pH 7.4 and processed for electron microscopy as detailed elsewhere [18].

Fluorescence microscopy. Cells were incubated for 45 min with 500 nM Mitotracker Red FM (Invitrogen) followed by staining with Hoechst (1 mg/ml) for 10 min at 37º C. Cellular fluorescence was analyzed in a Axiovert 200 (Zeiss) microscope using a ccd camera. The red fluorescence intensity of the cells was calculated using Image J.

Statistical analysis. Statistical analyses were performed using a two-tailed Student's t test. The results shown are the means±S.E.M. A $p<0.05$ was considered statistically significant.

Acknowledgements

Mrs. C. Núñez de Arenas and M. Chamorro are acknowledged for expert technical assistance. IMR, JGB and FS were supported by pre-doctoral fellowships from JAE-CSIC, FPI-MEC and FPI-UAM Spain, respectively. This work was supported by grants from the Ministerio de Educación y Ciencia (BFU2010-18903), the Centro de Investigación Biomédica en Red de Enfermedades Raras (CIBERER), ISCIII, and Comunidad de Madrid (S2011/BMD-2402), Spain. The CBMSO recieves an institutional grant from the Fundación Ramón Areces.

Author contributions: M.S-A and J.M.C. designed research; M.S-A., J.G-B. I.M-R. and F.S. performed research; M.S-A and J.M.C. analyzed data; M.S-A and J.M.C. wrote the paper.

Conflict of Interest: The authors declare no conflict of interest.

Supplementary information is available at EMBO *reports* Online´.

References

1. Gledhill JR, Montgomery MG, Leslie AG, Walker JE (2007) How the regulatory protein, IF(1), inhibits F(1)-ATPase from bovine mitochondria. *Proc Natl Acad Sci U S A* **104:** 15671-15676
2. Sanchez-Cenizo L, Formentini L, Aldea M, Ortega AD, Garcia-Huerta P, Sanchez-Arago M, Cuezva JM (2010) Up-regulation of the ATPase inhibitory factor 1 (IF1) of the mitochondrial H+-ATP synthase in human tumors mediates the metabolic shift of cancer cells to a Warburg phenotype. *J Biol Chem* **285:** 25308-25313
3. Formentini L, Sánchez-Aragó M, Sánchez-Cenizo L, Cuezva JM (2012) The mitochondrial ATPase Inhibitory Factor 1 (IF1) triggers a ROS-mediated retrograde pro-survival and proliferative response. *Mol Cell* **45:** 731-742
4. Rehman J (2010) Empowering self-renewal and differentiation: the role of mitochondria in stem cells. *J Mol Med* **88:** 981-986
5. Tormos KV, Anso E, Hamanaka RB, Eisenbart J, Joseph J, Kalyanaraman B, Chandel NS (2011) Mitochondrial complex III ROS regulate adipocyte differentiation. *Cell Metab* **14:** 537-544
6. Chen CT, Shih YR, Kuo TK, Lee OK, Wei YH (2008) Coordinated changes of mitochondrial biogenesis and antioxidant enzymes during osteogenic differentiation of human mesenchymal stem cells. *Stem Cells* **26:** 960-968
7. Folmes CD, Nelson TJ, Martinez-Fernandez A, Arrell DK, Lindor JZ, Dzeja PP, Ikeda Y, Perez-Terzic C, Terzic A (2011) Somatic oxidative bioenergetics transitions into pluripotency-dependent glycolysis to facilitate nuclear reprogramming. *Cell Metab* **14:** 264-271
8. Cuezva JM *et al* (2002) The bioenergetic signature of cancer: a marker of tumor progression. *Cancer Res* **62:** 6674-6681
9. Zhang J *et al* (2011) UCP2 regulates energy metabolism and differentiation potential of human pluripotent stem cells. *Embo J* **30:** 4860-4873
10. Willers IM, Cuezva JM (2011) Post-transcriptional regulation of the mitochondrial H(+)-ATP synthase: A key regulator of the metabolic phenotype in cancer. *Biochim Biophys Acta* **1807:** 543-551
11. Willers IM, Martínez-Reyes I, Martínez-Diez M, Cuezva J (2012) miR-127-5p targets the 3'UTR of human β-F1-ATPase mRNA and inhibits its translation. *Biochim Biophys Acta-Bioenergetics* **1817:** 838-848
12. Lawson DA, Xin L, Lukacs RU, Cheng D, Witte ON (2007) Isolation and functional characterization of murine prostate stem cells. *Proc Natl Acad Sci U S A* **104:** 181-186
13. Olsen Hult LT, Kleiveland CR, Fosnes K, Jacobsen M, Lea T (2011) EP receptor expression in human intestinal epithelium and localization relative to the stem cell zone of the crypts. *PLoS One* **6:** e26816
14. Scarpulla RC (2008) Transcriptional paradigms in mammalian mitochondrial biogenesis and function. *Physiol Rev* **88:** 611-638
15. Birket MJ, Orr AL, Gerencser AA, Madden DT, Vitelli C, Swistowski A, Brand MD, Zeng X (2011) A reduction in ATP demand and mitochondrial activity with neural differentiation of human embryonic stem cells. *J Cell Sci* **124:** 348-358
16. Ramanathan A, Wang C, Schreiber SL (2005) Perturbational profiling of a cell-line model of tumorigenesis by using metabolic measurements. *Proc Natl Acad Sci U S A* **102:** 5992-5997
17. Cai N, Li M, Qu J, Liu GH, Izpisua Belmonte JC (2012) Post-translational modulation of pluripotency. *J Mol Cell Biol* **4:** 262-265

18. Sanchez-Arago M, Chamorro M, Cuezva JM (2010) Selection of cancer cells with repressed mitochondria triggers colon cancer progression. *Carcinogenesis* **31:** 567-576
19. Martinez-Reyes I, Sanchez-Arago M, Cuezva JM (2012) AMPK and GCN2-ATF4 signal the repression of mitochondria in colon cancer cells. *Biochem J* **444:** 249-259

Figure legends

Figure 1. Metabolic reprogramming of stem cells upon osteogenic differentiation. hMSCs were grown in the osteogenic induction media to promote differentiation**. (A)** Representative images of undifferentiated stem cells (hMSCs) and osteocytes. **(B)** Western blots of the expression of CD44, osteopontin and tubulin in two different preparations of hMSCs and osteocytes (Ost.). The histograms show the calculated osteopontin/CD44 ratio. Bars are the mean ± S.E.M of four different samples. *, $p<0.05$ when compared to hMSCs. **(C)** hMSCs and osteocytes were processed for the determination of the rates of aerobic glycolysis in the absence (-) or presence (+) of 6μM oligomycin (OL). Bars are the mean ± S.E.M. of 6-10 independent determinations. *, $p<0.05$ when compared to OL-untreated cells. **(D)** The rates of basal respiration were determined in hMSCs and osteocytes. OL-sensitive respiration (OSR) and maximum respiratory rates (MRR) were also measured after the addition of 6μM OL and 0.75 mM DNP, respectively. Bars represent the mean ± S.E.M. of three independent experiments. *, $p<0.05$ when compared to hMSCs. **(E)** Cellular ATP concentrations were determined in the absence (-) or presence (+) of 6μM OL. Bars are the mean ± S.E.M. of three different experiments.*, $p<0.05$ when compared to OL-untreated cells.

Figure 2. Differentiation of mitochondria upon osteogenic induction. (A) Representative western blots of the expression of mitochondrial proteins (NADHs9, NDUFS3, SDH-B, Core 2, COXI, COX II, COXIV, α-F1ATPase, β-F1ATPase, HADHA, Hsp60 and VDAC), glycolytic enzymes (GAPDH, PK-M2, and LDH-A) and tubulin in two different preparations of hMSCs and osteocytes. **(B)** hMSCs and osteocytes were processed for the determination of the relative mtDNA copy number (12S/β-F1-ATPase ratio). Bars represent the mean ± S.E.M. of seven independent

determinations. **(C)** The mitochondrial mass was determined by the content of cardiolipin as assessed by NAO fluorescence. Bars are the mean ± S.E.M of six independent determinations. *, $p<0.05$ when compared to hMSCs. **(D)** Fluorescence microscopy of hMSC and osteocytes stained with MitoTracker Red and Hoechst. Images reveal a partially fragmented mitochondrial network in hMSCs when compared to the thread-like morphology of mitochondria observed in osteocytes. The histogram shows the quantification of the MitoTracker signal in hMSCs and osteocytes. The results shown are the mean ± S.E.M of 45-60 different cells. a.u, arbitrary units. **(E)** Representative electron microscopy images of mitochondria in hMSCs and osteocytes. Onion-like mitochondria (white arrows) are observed in hMSCs. The histograms show the quantification of the number of mitochondria per cell section and the percentage of abnormal organelles in ultrathin sections of hMSCs and osteocytes, respectively. The results shown are the mean ± S.E.M of 45-50 different cells. *, $p<0.05$ when compared to hMSCs. **(F)** The histogram shows the mean ±S.E.M of the calculated β-F1-ATPase/Hsp60 ratio in hMSCs and osteocytes in four different samples. *, $p<0.05$ when compared to hMSCs.

Figure 3. IF1 degradation mediates metabolic reprogramming of stem cells during osteogenic differentiation. (A) Representative blots of IF1 and tubulin in two different preparations of hMSCs and osteocytes. Osteogenic induction is accompanied by repression of IF1 expression. **(B-D, H)** hMSCs were transfected with control (siCRL, closed bars) or siIF1 siRNA (siIF1, hatched bars) to regulate the expression of IF1. **(B)** Shows the rates of aerobic glycolysis in the absence (-) or presence (+) of 6 μM OL. Bars are the mean ± S.E.M. of 6 independent determinations. *, and #, $p<0.05$ when compared to siCRL or siIF1 untreated cells, respectively. **(C)** The rates of OL-sensitive

respiration (OSR) were determined after addition of 6 μM OL. Data are shown as percentage of the basal respiration. Bars are the mean ± S.E.M. of eight independent determinations. *, $p<0.05$ when compared to siCRL. **(D)** Cellular ATP concentrations were determined in the absence (-) or presence (+) of 6 μM OL. Bars are the mean ± S.E.M. of twelve independent determinations. *, $p<0.05$ when compared to OL-untreated cells. **(E)** IF1 mRNA expression was assessed by RT-qPCR in hMSCs and osteocytes. Bars are the mean ± S.E.M. of six independent determinations. **(F)** hMSCs and osteocytes were treated twenty-four hours with (+) or without (-) 400μM of the serine-protease inhibitor AEBSF to block the activity of mitochondrial proteases, and the expression of IF1 and β-actin (loading control) analyzed by western blot in two different preparations. Plots are the mean ± S.E.M. of the calculated IF1/β-actin ratio in four different experiments.*, $p<0.05$ when compared to untreated (-) cells. **(G)** The rates of aerobic glycolysis in the absence (-) or presence (+) of 400μM of AEBSF or 6μM OL were determined in hMSCs and osteocytes. Bars are the mean ± S.E.M. of 6 independent determinations.*, $p<0.05$ when compared to untreated cells. **(H)** The expression of CD44 and osteopontin was analyzed by western blot at the indicated times to asses the rate of differentiation after silencing of IF1. The plot represents the calculated osteopontin/CD44 ratio in siCRL and siIF1 cells. *, $p<0.05$ when compared to siCRL.

Figure 4. IF1 is a stem cell marker. (A) Immunohistochemistry of IF1 expression in human normal and tumor prostate and colon tissues. Images are shown at 20-40X magnification **(B)** Double-immunofluorescence microscopy of normal human prostate and colon stained with CD44 antibody (green) and with monoclonal IF1 antibody (red). The merged images revealed the co-localization of IF1 in stem cells niches of both

tissues. Images are shown at 40X magnification. **(C)** Scheme of the proposed mechanism by which IF1 (dark blue) regulates metabolic rewiring upon cellular differentiation / dedifferentiation. Stem and cancer cells (dark yellow) show a high expression of IF1 which promotes the inhibition of OXPHOS favoring aerobic glycolysis. Differentiation triggers an enhanced degradation of IF1 (+, green) and the activation of OXPHOS in the differentiated cell (light blue). The relevance of glycolysis as ATP supplier is diminished in this situation. Dedifferentiation of somatic cells into cancer cells results in the accumulation of IF1, the inhibition of OXPHOS and the activation of aerobic glycolysis. The accumulation of IF1 in cancer cells might be regulated by inhibiting the degradation of the protein (-, red).

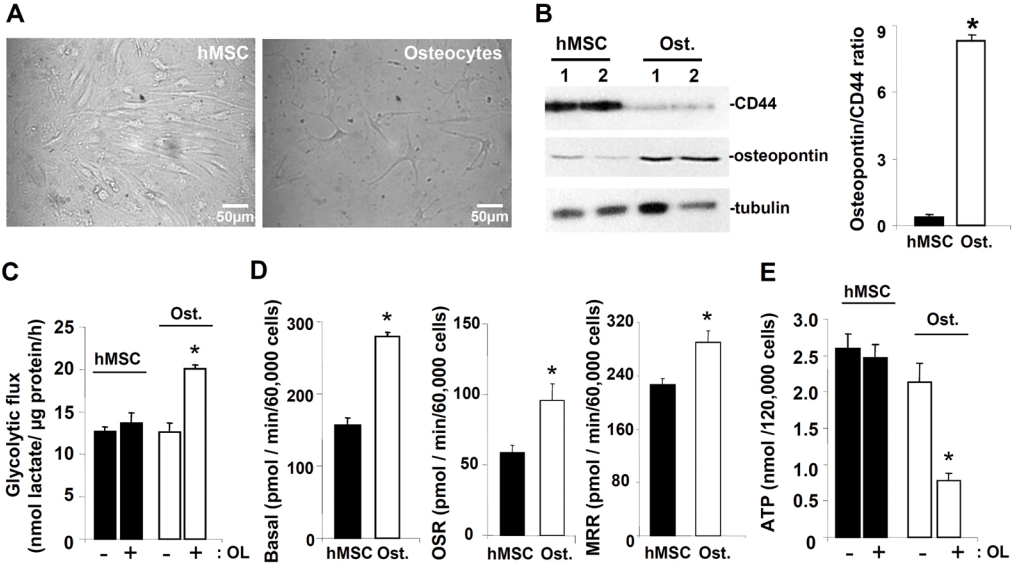
A
hMSC
Osteocytes
50μm
50μm
B
hMSC
Ost.
1
2
1
2
-CD44
-osteopontin
-tubulin
Osteopontin/CD44 ratio
9
6
3
0
*
hMSC
Ost.
C
Glycolytic flux
(nmol lactate/ μg protein/h)
25
20
15
10
5
0
hMSC
Ost.
*
- + - + : OL
D
Basal (pmol / min/60,000 cells)
300
200
100
0
*
hMSC Ost.
OSR (pmol / min/60,000 cells)
150
100
50
0
*
hMSC Ost.
MRR (pmol / min/60,000 cells)
320
240
160
80
0
*
hMSC Ost.
E
ATP (nmol /120,000 cells)
3.0
2.5
2.0
1.5
1.0
0.5
0
hMSC
Ost.
*
- + - + : OL

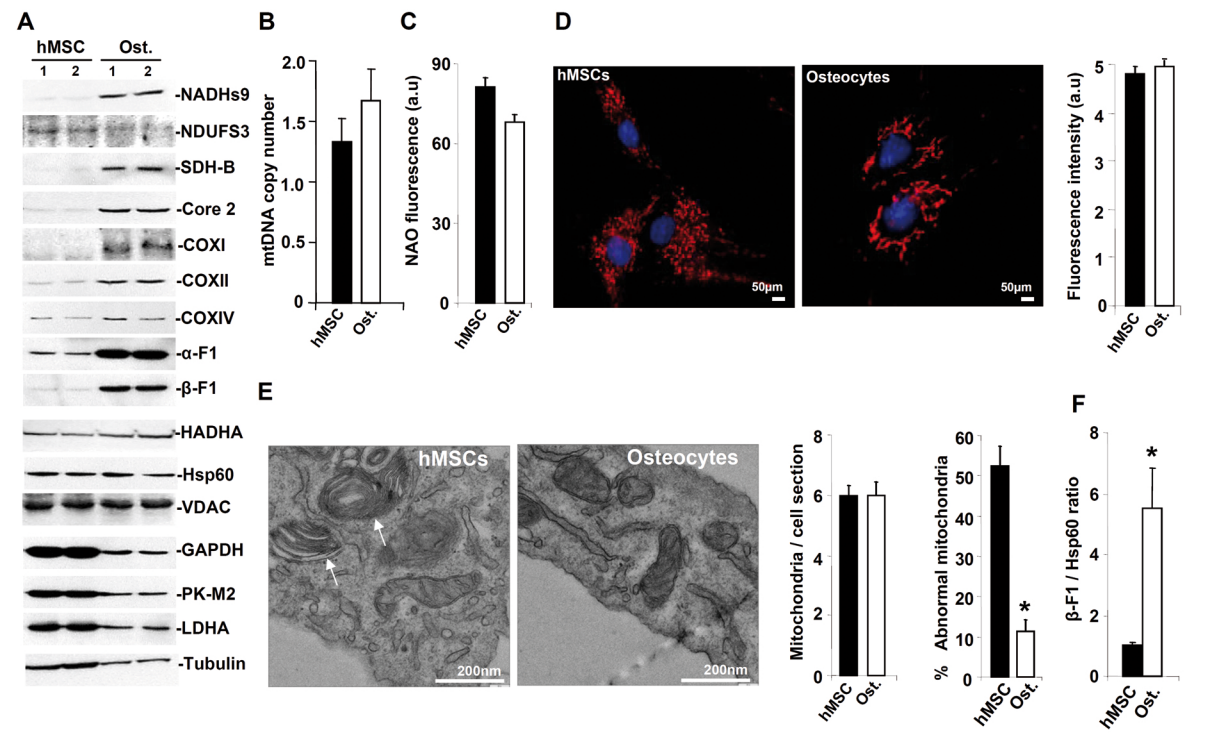
A
hMSC
Ost.
1
2
1
2
-NADHs9
-NDUFS3
-SDH-B
-Core 2
-COXI
-COXII
-COXIV
-α-F1
-β-F1
-HADHA
-Hsp60
-VDAC
-GAPDH
-PK-M2
-LDHA
-Tubulin
B
mtDNA copy number
2.0
1.5
1.0
0.5
0
hMSC
Ost.
C
NAO fluorescence (a.u)
90
60
30
0
hMSC
Ost.
D
hMSCs
Osteocytes
50μm
50μm
Fluorescence intensity (a.u)
5
4
3
2
1
0
hMSC
Ost.
E
hMSCs
Osteocytes
200nm
200nm
Mitochondria / cell section
8
6
4
2
0
hMSC
Ost.
% Abnormal mitochondria
60
50
40
30
20
10
0
*
hMSC
Ost.
F
β-F1 / Hsp60 ratio
8
6
4
2
0
*
hMSC
Ost.

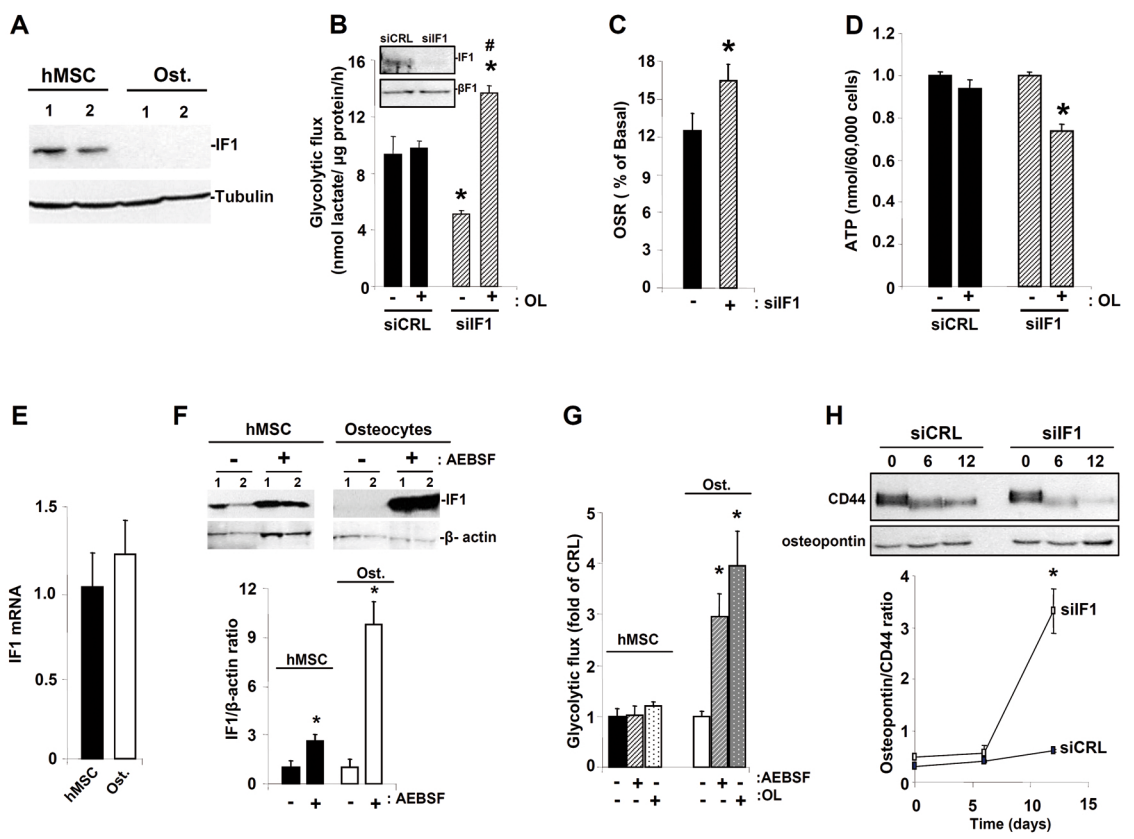
A
hMSC
Ost.
1
2
1
2
-IF1
-Tubulin
B
siCRL
siIF1
IF1
βF1
#
*
Glycolytic flux
(nmol lactate/ μg protein/h)
16
12
8
4
0
*
*
-
+
-
+
: OL
siCRL
siIF1
C
OSR (% of Basal)
18
15
12
9
6
3
0
*
-
+
: siIF1
D
ATP (nmol/60,000 cells)
1.2
1.0
0.8
0.6
0.4
0.2
0
*
-
+
-
+
: OL
siCRL
siIF1
E
IF1 mRNA
1.5
1.0
0.5
0
hMSC
Ost.
F
hMSC
Osteocytes
-
+
-
+
: AEBSF
1
2
1
2
1
2
1
2
-IF1
-β- actin
IF1/β-actin ratio
12
9
6
3
0
Ost.
*
*
hMSC
*
-
+
-
+
: AEBSF
G
Glycolytic flux (fold of CRL)
5
4
3
2
1
0
Ost.
*
*
*
hMSC
-
+
-
-
+
-
:AEBSF
-
-
+
-
-
+
:OL
H
siCRL
siIF1
0
6
12
0
6
12
CD44
osteopontin
Osteopontin/CD44 ratio
4
3
2
1
0
*
siIF1
siCRL
0
5
10
15
Time (days)

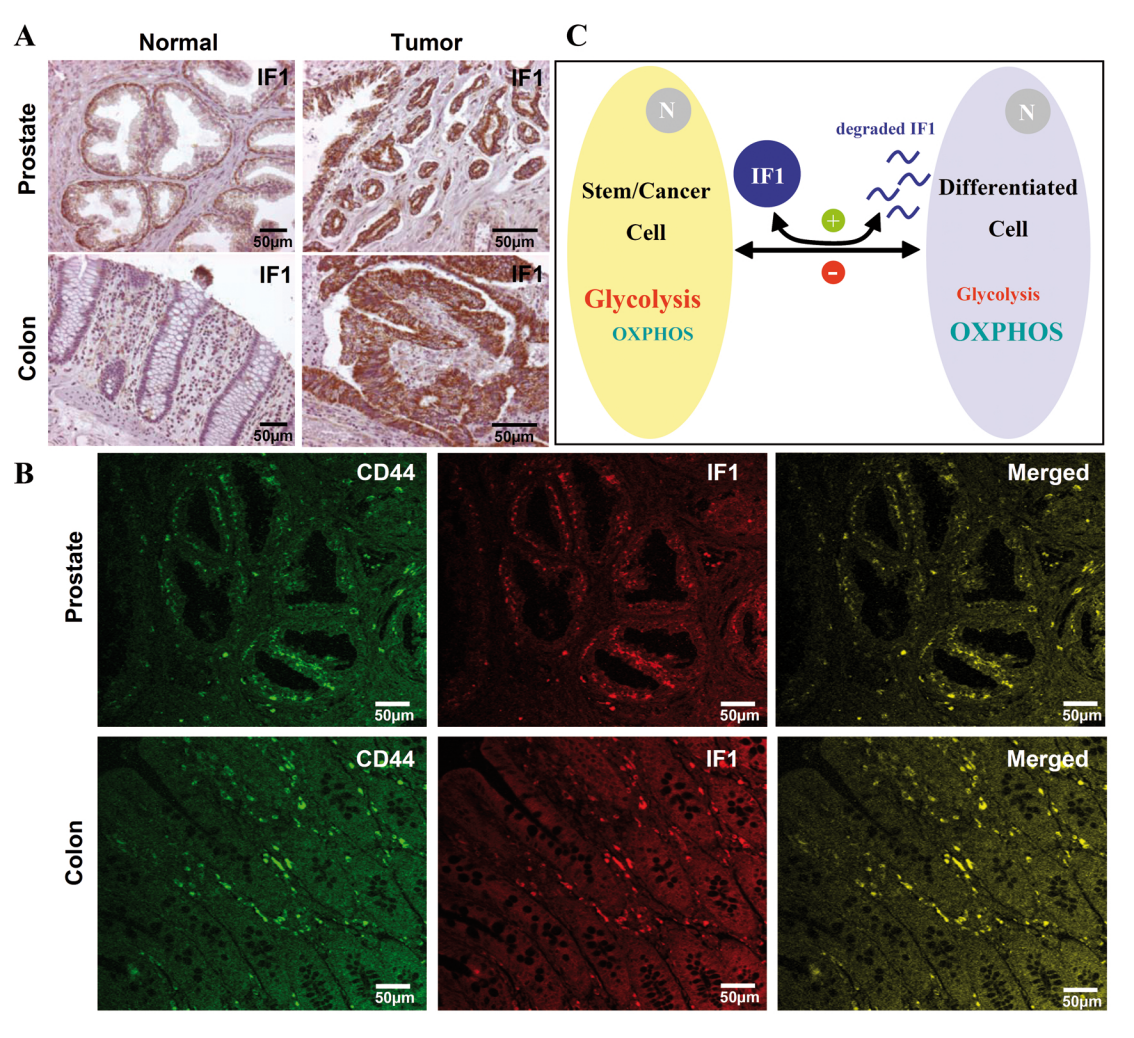
A
Normal
Tumor
Prostate
Colon
IF1
50μm
C
N
Stem/Cancer Cell
Glycolysis
OXPHOS
IF1
degraded IF1
+
-
Differentiated Cell
Glycolysis
OXPHOS
B
CD44
IF1
Merged
Prostate
Colon
50μm

Supporting Information.

Degradation of IF1 controls energy metabolism during osteogenic differentiation of stem cells

María Sánchez-Aragó[1], Javier García-Bermúdez[1], Inmaculada Martínez-Reyes[1], Fulvio Santacatterina[1] and José M. Cuezva[1, *]

Supporting Results

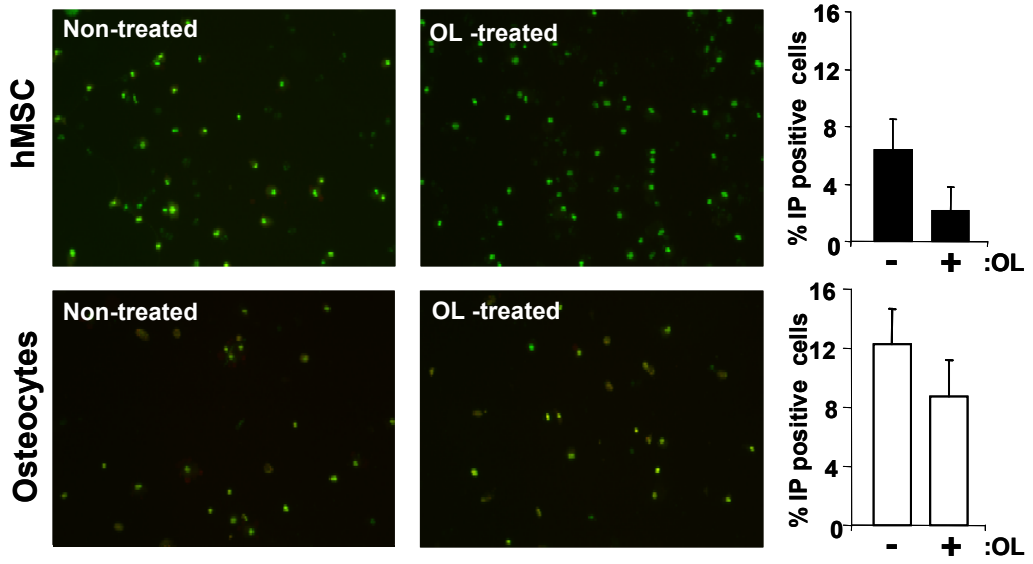

Figure S1. Oligomycin (OL) treatment has no effect on cell death in hMSCs and osteocytes. Cells were exposed to 6 μM OL or left untreated. Cells were double-stained with Hoechst 33342 (green) and propidium iodide (PI, red) and visualized using fluorescence microscopy at 20x magnification. The percentage of PI positive cells (dead cells) was determined by examination of 10 different fields taken at random. Histograms are the means ± S.E.M.

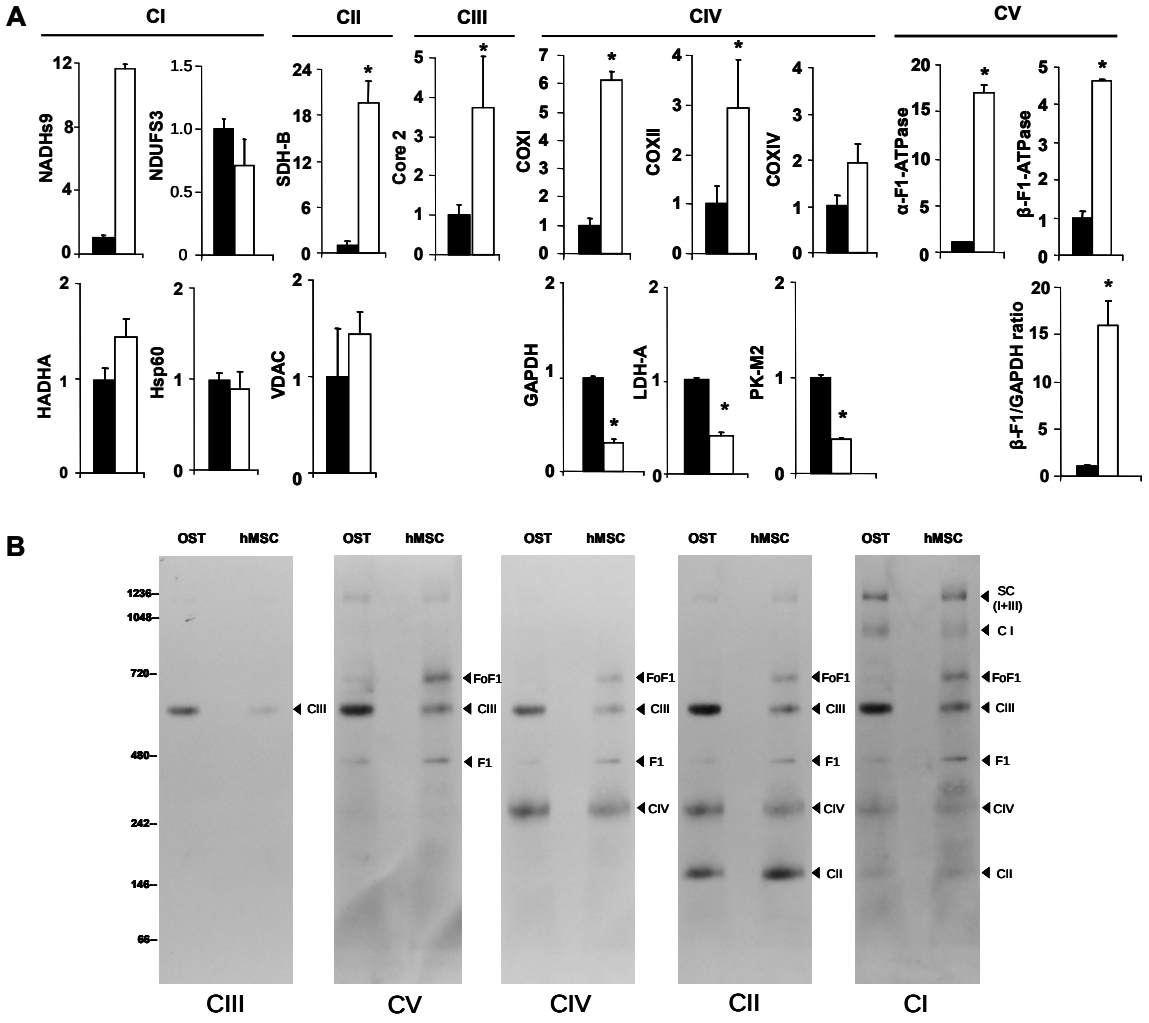

Figure S2. Differentiation of mitochondria upon osteogenic induction. A. Histograms show the quantification of the expression of mitochondrial (NADHs9, NDUFS3, SDH-B, Core 2, COXI, COXII, COXIV, α-F1-ATPase, β-F1-ATPase, HADHA, Hsp60 and VDAC) and glycolytic (GAPDH, LDH-A and PK-M2) enzymes in hMSCs (closed bars) and osteocytes (open bars) (for representative blots see Fig. 2A). The bioenergetic signature (β-F1/GAPDH ratio) in hMSCs and osteocytes is also shown. Data are expressed as fold change relative to the values in hMSCs. Bars represent the mean ± S.E.M. of four different preparations.*, $p<0.05$ when compared to hMSCs. **B.** Analysis of OXPHOS complexes by BN-PAGE in the presence of *n*-dodecyl β-D-maltoside from digitonin-enriched mitochondrial membranes from hMSC and osteocytes (OST). A representative experiment is shown. The membrane has been sequentially blotted with antibodies against complex III (CIII), complex V (F0F1), complex IV (CIV), complex II (CII) and complex I (CI). The migration of F1-ATPase (F1), supercomplex I+III (SC I+III) and of molecular mass markers (kDa) is also indicated.

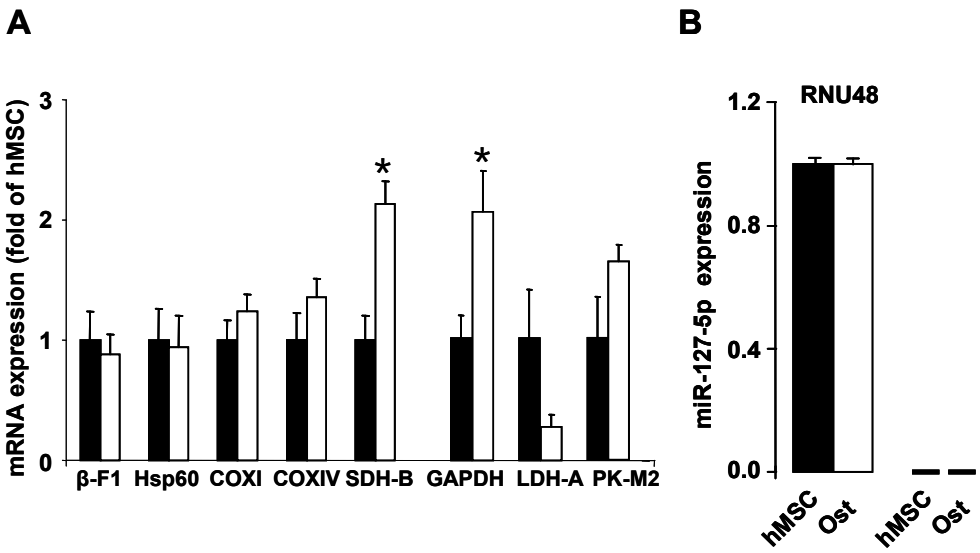

Figure S3. Post-transcriptional regulation of mitochondrial differentiation. Total RNA was extracted from hMSC (closed bars) and osteocytes (open bars). (**A**) Expression of representative mitochondrial (β-F1-ATPase, Hsp60, COXIV, COXI, and SDH-B) and glycolytic (GAPDH, LDH-A and PK-M2) mRNAs was assessed by RT-qPCR. Histograms show the mean ± S.E.M. of six different determinations. *, $p<0.05$ when compared to hMSCs. (**B**) Quantification of miR-127-5p by RT-qPCR in hMSCs and osteocytes. RNU48 values are shown to highlight the negligible expression of miR-127-5p in both undifferentiated and differentiated cells. Bars are the mean ± S.E.M. of 3 independent determinations.

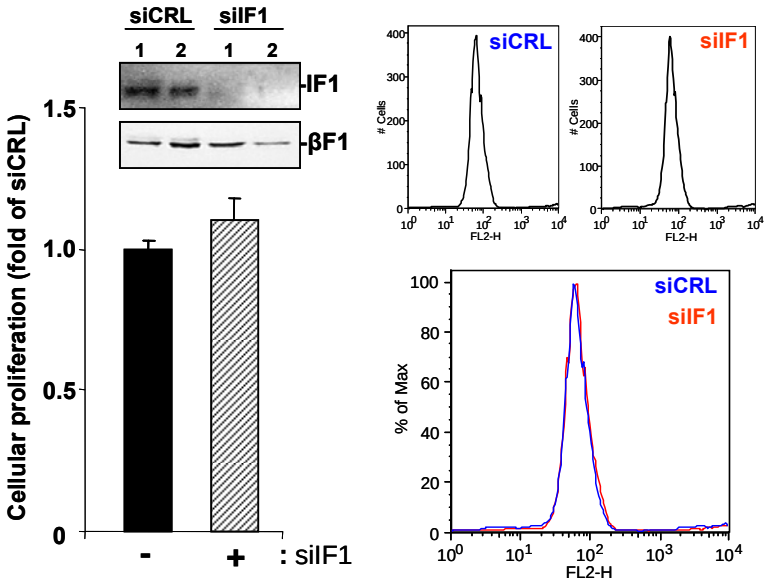

Figure S4. IF1 is not signaling cellular proliferation in hMSC. hMSCs were transfected with control (siCRL, closed bars) or siIF1 siRNA (siIF1, hatched bars) to regulate the expression of IF1. Cellular proliferation was assessed by the incorporation of EdU into cellular DNA. Blue (Control, siCRL) and red (siIF1) traces are shown. Bars are the mean ± S.E.M. of 6 independent determinations. Data are shown as fold change relative to the values in siCRL cells.

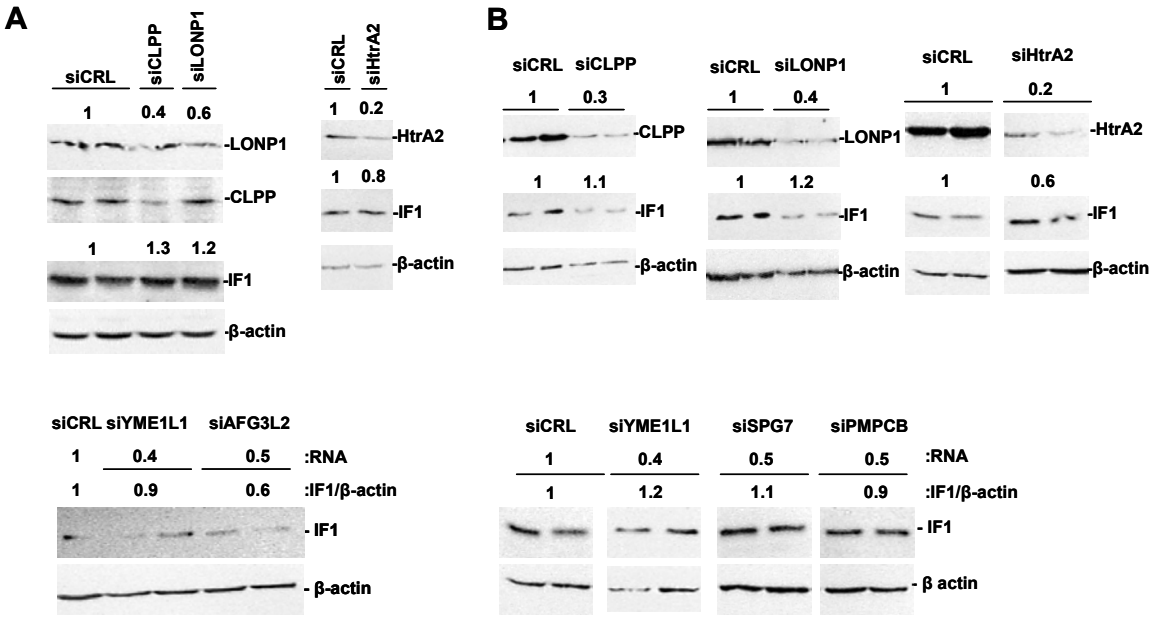

Figure S5. siRNA screening for the putative protease involved in the degradation of IF1. hMSCs **(A)** and HCT116 colon cancer cells **(B)** were transfected for 48 hours with 80-100 nM siCRL or with the specified siRNA for the following mitochondrial proteases: AFG3L2, CLPP, HtrA2, LONP1, PMPCB, SPG7 and YME1L1. Representative blots of IF1 and β-actin are shown. The calculated IF1/β-actin ratio is indicated on top of the blots. Silencing of CLPP, HtrA2 and LONP1 was verified by western blotting and the degree of silencing indicated on top of the blots. Silencing of AFG3L2, PMPCB, SPG7 and YME1L1 was verified by RT-qPCR and indicated.

Supporting Methods

Osteogenic induction and treatments. To induce osteogenic differentiation, hMSCs were incubated in the osteogenic media containing dexamethasone, ascorbate, Mesenchymal Cell Growth Supplement, L-glutamine, penicillin/streptomycin and β-glycerophosphate (Lonza). For inhibition of mitochondrial serine-proteases, hMSC and osteocytes were treated with 400μM of 4-(2-aminoethyl) benzenosulfonyl fluoride hydrochloride (AEBSF) for the indicated time.

Antibodies used: anti-CD44 (1:1,000) from Millipore; anti-β-F1-ATPase (1: 25,000) [1]; anti-IF1 (1:200) [2]; anti-PK-M2 (pyruvate kinase M2) (1:1000); anti-NADHs9 (NADH dehydrogenase subunit 9) (1:1,000); anti-GAPDH (1:20,000); anti-LDH-A (1:1,1000) [3]; anti-Hsp60 (Heat Shock Protein) (Stressgene SPA-807, 1:2,000); anti-SDH-B (succinate dehydrogenase subunit B) (1:500) and anti-COXIV (cytocrome c

oxidase subunit IV (1:250) from Invitrogen; anti-α-F1-ATPase (α-F1-ATPase) (1:1,000) from Molecular Probes; anti-osteopontin (1:1,000), anti-NDUFS3 of complex I (1:1,000), anti-Core 2 of complex III (1:500), anti-MTCO2 (cytocrome c oxidase subunit II) (1:500), anti-MTCO1 (cytocrome c oxidase subunit I) (1:100), anti-VDAC1 (porin) (1:500), anti-LONP1 antibody (1:250) and anti-CLPP (1:200) from Abcam; anti-Htra2/Omi (1:500) from Cell Signaling; anti-tubulin (1:5,000) and anti-β-actin (1:100,000) from Sigma. Peroxidase-conjugated anti-mouse and anti-rabbit IgGs (Nordic Immunonology, 1: 3,000) were used as secondary antibodies. The blots were developed using the ECL reagent. Quantification of the immunoreactive bands was accomplished using a Kodak DC120 Zoom digital camera and the Kodak 1D Image Analysis Software for Windows. The ratios β-F1-ATPase/Hsp60 and β-F1-ATPase/GAPDH were taken as respective indexes of the bioenergetic competence of the organelle (mitochondrial differentiation) and of the overall mitochondrial activity in the cell (that results from both mitochondrial proliferation and differentiation), and illustrate the two main pathways that restrain the bioenergetic activity of mitochondria in cancer cells [1, 4].

siRNA silencing. Transfections were performed using Lipofectamine and Plus Reagent (Invitrogen™). Suppression of IF1 (Qiagen S100908075) expression was exerted by small interfering RNA (siRNA). An inefficient siRNA sequence, Silencer® Select Negative Control #1 plasmid (Ambion/Applied Biosystems), was used as a control. Suppression of expression of mitocondrial proteases was exerted using the following Silencer Select siRNAs (Invitrogen): LONP1 (s17903), CLPP (s15686), HTRA2 (s653), AFG3L2 (s21516), SPG7 (s224671), PMPCB (s18239), YME1L1 (s21077). Silencer Negative Control siRNA #1 (AM4636) was used as control. Silencing was verified by western blotting (LONP1/CLPP/HTRA2) or by RT-qPCR (AFG3L2/SPG7/PMPCB/YME1L1). The forward (F) and reverse (R) primers used were: β-actin, F: 5'- CCAACCGCGAGAAGATGA-3', R: 5'-CCAGAGGCGTACAGGGATAG-3'; PMPCB, F: 5'-TGCCAGCTTGCTGTTTAATG-3', R: 5'-TTGCCTCTTTTATGGAAATGG-3'; YME1L1, F: 5'-CATGGTGGCAGGTGCTTAT-3', R: 5'-CTCCATCTCCCAGGCTCA-3'; SPG7, F: 5'-GTCCGGCTTCTCCAACAC-3', R: 5'-AGGGTAGCTGGTCAAGAGAGG-3'; AFG3L2, F: 5'-GAGGAAGAGGCAACTTTGGA-3', R: 5'AATGACGACATTTGTTGTTGTATTAAA-3'.

Immunohistochemistry. Formalin-fixed, paraffin-embedded normal and tumor 5 μm sections of human colon and prostate biopsies were used (Origene). Sections were deparaffined and the antigens retrieved by incubation in EDTA for 45 min at 155ºC. The monoclonal anti-IF1 (1:200) antibody was used as detailed [5]. Sections were counterstained with hematoxylin.

Immunofluorescence microscopy. For co-localization studies, deparaffinated normal human colon and prostate 5 μm tissue sections were used. The primary antibodies used were anti-CD44 (1:50) and anti-IF1 (1:50) [2]. Slides were incubated for 2h in the dark with anti-(rabbit) and anti-(mouse) IgGs conjugated to Alexa Fluor® 488 and 555, respectively. Cellular fluorescence was analyzed by confocal microscopy in a LSM510 META (Zeiss).

Gene expression analysis by RT-qPCR. Total RNA was extracted from cell cultures using TRIzol Reagent (Invitrogen) or RNAeasy Mini Kit (QIAgen). RNA was quantified with a Nanodrop ND-1000 spectrophotometer. RNA integrity was assessed with an Agilent 2100 Bioanalyzer. Reverse transcription (RT) reactions were performed using 1 μg of total RNA and the High Capacity Reverse Transcription Kit (Applied Biosystems) with random primers, following manufacturer's instructions. Real-time PCR was performed using Power Sybr Green PCR Master Mix with an ABIPRISM 7900HT instrument (Applied Biosystems). The expression level of indicated mRNAs was determined according to the ΔΔCt method using β-actin as internal control.

Assessment of cellular proliferation. The incorporation of 5-ethynyl-2´deoxy-uridine (EdU) into cellular DNA was determined using the Click-iT EdU Flow Cytometry Assay Kit (Molecular Probes) [5].

Cell death assays. Cells were harvested, washed with PBS and incubated in the dark for 5 min with Hoechst 33342 (1mg/mL) and propidium iodide (1mg/mL) solutions. After washing, samples were observed under a Leica DM-IRB fluorescence microscope (UV). The percentage of dead (red staining) cells was calculated from 10 different randomly selected fields for each condition assayed.

Blue native electrophoresis (BN)-PAGE. Enriched mitochondrial fractions were isolated from cell cultures using digitonin [6]. Protein extracts were solubilized in BN-loading buffer (1.5 M 6-aminocaproic acid, 50 mM Bis-Tris/HCl pH 7.0) in the presence of 2 μl PMSF/0.5 mM DMSO. *n*-dodecyl β-D-maltoside at the concentration of 3 g/g protein was added to the samples and incubated on ice for 10 min. Solubilized samples were centrifuged for 30 min at 30,000 rpm at 4ºC, and the supernatant was

combined with 2 µl of sample buffer (500 mM aminocaproic acid, 50 mM Bis-Tris/HCl pH 7.0, 0.5 mM EDTA, 5% Serva Blue G-250) prior to loading in 3-13% gradient gels [7].

Supporting References

1. Cuezva JM *et al* (2002) The bioenergetic signature of cancer: a marker of tumor progression. *Cancer Res* **62:** 6674-6681

2. Sanchez-Cenizo L, Formentini L, Aldea M, Ortega AD, Garcia-Huerta P, Sanchez-Arago M, Cuezva JM (2010) Up-regulation of the ATPase inhibitory factor 1 (IF1) of the mitochondrial H+-ATP synthase in human tumors mediates the metabolic shift of cancer cells to a Warburg phenotype. *J Biol Chem* **285:** 25308-25313

3. Acebo P *et al* (2009) Cancer abolishes the tissue type-specific differences in the phenotype of energetic metabolism. *Transl Oncol* **2:** 138-145

4. Cuezva JM, Ortega AD, Willers I, Sanchez-Cenizo L, Aldea M, Sanchez-Arago M (2009) The tumor suppressor function of mitochondria: translation into the clinics. *Biochim Biophys Acta* **1792:** 1145-1158

5. Formentini L, Sánchez-Aragó M, Sánchez-Cenizo L, Cuezva JM (2012) The mitochondrial ATPase Inhibitory Factor 1 (IF1) triggers a ROS-mediated retrograde pro-survival and proliferative response. *Mol Cell* **45:** 731-742

6. Calvaruso MA, Smeitink J, Nijtmans L (2008) Electrophoresis techniques to investigate defects in oxidative phosphorylation. *Methods* **46:** 281-287

7. Schägger H (2003) Membrane Protein Purification and Crystallization: A Practical Guide. Elsevier Science, USA.